A technique to obtain a multiparameter radar rainfall algorithm using the probability matching procedure (*)

E. GORGUCCI ([1]), G. SCARCHILLI ([1]) and V. CHANDRASEKAR ([2])

([1]) *Istituto di Fisica dell'Atmosfera* (*CNR*) - *Roma, Italy*
([2]) *Colorado State University - Fort Collins, Colorado, USA*

(ricevuto il 16 Novembre 1995; revisionato il 30 Luglio 1996; approvato l'11 Novembre 1996)

Summary. — The natural cumulative distributions of rainfall observed by a network of rain gauges and a multiparameter radar are matched to derive multiparameter radar algorithms for rainfall estimation. Conventional usage of multiparameter radar measurements for rainfall estimation has been associated with tracking the variability of the raindrop size distribution. The use of multiparameter radar measurements in a statistical framework to estimate rainfall is presented in this paper. The techniques developed in this paper are applied to the radar and rain gauge measurement of rainfall observed in central Florida and central Italy. Conventional pointwise estimates of rainfall are also compared. The probability matching procedure, when applied to the radar and surface measurements, shows that multiparameter radar algorithms can match the probability distribution function better than the reflectivity-based algorithms, thereby indicating the potential of multiparameter radar measurements for statistical approach to rainfall estimation. It is also shown that the multiparameter radar algorithm derived matching the cumulative distribution function of rainfall provides more accurate estimates of rainfall on the ground in comparison to any conventional reflectivity-based algorithm.

PACS 92.60.Jq – Water in the atmosphere (humidity, clouds, evaporation, precipitation).

1. – Introduction

There have been two general approaches to estimate rainfall using radar, namely: *a*) those that obtain an instantaneous point estimate in space and *b*) those that provide climatological estimates over large areas. Most of the studies on the statistical techniques for obtaining the mean estimate of rainfall use the reflectivity factor only [1] and the majority of the studies in the area of rainfall estimation using polarimetric techniques have been concentrating on instantaneous spatial estimates of rainfall [2]. Conventionally all the multiparameter researches have been associated with those studying the variability in the raindrop size distribution [3, 4]. However, extensive observation of multiparameter signatures in tropical and subtropical

(*) The authors of this paper have agreed to not receive the proofs for correction.

environments suggests that those storms are rich in polarimetric signatures [5]. Therefore, inclusion of polarimetric signatures in a mean probability sense seems reasonable. In this paper we follow a new approach to obtain polarimetric radar estimates of rainfall. Historically, polarimetric radar techniques have all been branded as those that solve for variabilities in raindrop size distribution. However, in this paper we have tried to address a different question. Polarimetric radars provide alternate measurements, compared to reflectivity factor, that have different statistical spatial and temporal covariance structure. Therefore, polarimetric measurements have the potential to add additional information in the context of rainfall estimation. In this paper we evaluate whether the polarimetric measurements have something to add "in a statistical sense" to the problem of rainfall estimation.

Only a handful of experiments conducted very precisely have been able to demonstrate the improvements in multiparameter rainfall estimates [2]. Even these experiments have not shown improvements of the order predicted by theory owing to experimental limitations [6, 7]. Our approach does not treat the problem of multiparameter rainfall estimation as one that accounts for variability in DSD, but treats it in a statistical framework, formulated in a way so that it can use the wealth of polarimetric signatures present in rainstorms. We have adapted the probability distribution function matching approach discussed by Calheiros and Zawadzki [1] for multiparameter radar applications. In addition, we use the rainfall estimate obtained from the radar rainfall algorithms which are given by the probability matching procedure for comparison between radar and rain gauges. We utilize data from two geographic locations and two different radar systems operating at two different frequencies to evaluate our procedure. Dual polarization *S*-band radar data over Kennedy Space Center in Florida (USA) and dual polarization *C*-band radar data over the Arno river basin in Italy are analyzed in this paper.

Our paper is organized as follows: Section **2** describes the experimental set up of the two data sets. Section **3** discusses the dual polarization radar estimates of rainfall. Section **4** introduces the procedure for matching the probability density function of rainfall rates obtained by multiparameter radar and rain gauge. Section **5** summarizes the key results of this paper.

2. – Data sources and instrumentation

2˙1. CaPE *experiment*. – The instrumentation for rainfall measurement experiment during CaPE [8] primarily consisted of the CP-2 multiparameter radar and a network of rain gauges called TRMM rain gauges (name after the Tropical Rainfall Measurement Mission) located primarily in the vicinity of the Merrit island area at the Kennedy Space Center (KSC). Figure 1 shows the location of the CP-2 radar and the TRMM rain gauge network. The TRMM rain gauge network consists of 22 tipping bucket rain gauges with a recording resolution of 1 min located at NASA/KSC and CaPE Canaveral Airforce Station (CCAFS). The parameters of interest for precipitation measurement that were measured by the CP-2 radar were the reflectivity factor at horizontal polarization (Z_{H}) and the differential reflectivity (Z_{DR}), both measured at the *S*-band frequency. Table I lists the main features of the CP-2 radar that are relevant to this paper. Data used in this paper for rainfall measurement were collected integrating 64 samples pairs with 1 ms PRT (Pulse Repetition Time) in a PPI (Plan Position Indicator) mode with a typical scan rate of 8 degrees s^{-1}.

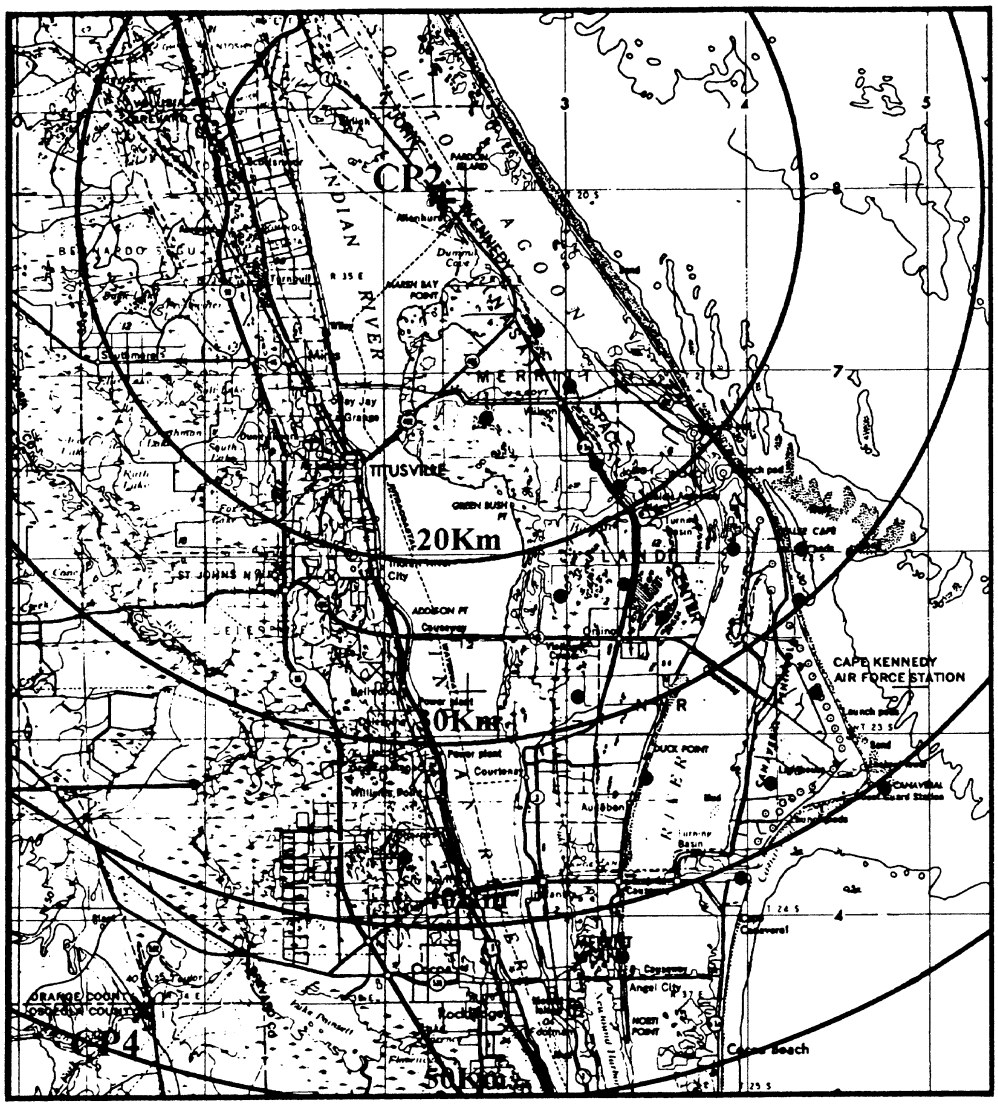

Fig. 1. – The location of CP-2 radar and rain gauge network during CaPE.

On July 26, 1991 the CP-2 radar began operating early and there was little activity during the morning. During the afternoon a cluster of storms moved over the TRMM rain gauge network and the thunderstorm activity lasted for about one hour. The CP-2 radar collected data over these storms in a PPI mode obtaining data over the rain gauge network.

2'2. *Data description from Polar* 55C. – The radar Polar 55C is located at Montagnana near Florence, Italy, to provide good radar coverage over the Arno river basin. Figure 2 shows the regional map with the radar location. The Polar 55C is a dual polarized pencil beam weather radar with a 0.9° beamwidth. The radar signals are

TABLE I. – *The characteristics of the* CP-2 *S-band radar.*

Characteristics	CP-2 radar *S*-band
Polarization type	linear
Wavelength (cm)	10.7
Peak power (kW)	1200
Pulse length (μs)	1.0
PRF (s^{-1})	960
Antenna type	center fed paraboloid
Antenna size (m)	8.5
Beamwidth	0.93°
Polarizations transmitted	linear *V* or *H*
Polarization received	copolar to transmit
Maximum sidelobe level (dB)	−21
Polarization control method	ferrite switch
Polarization control period	pulse by pulse

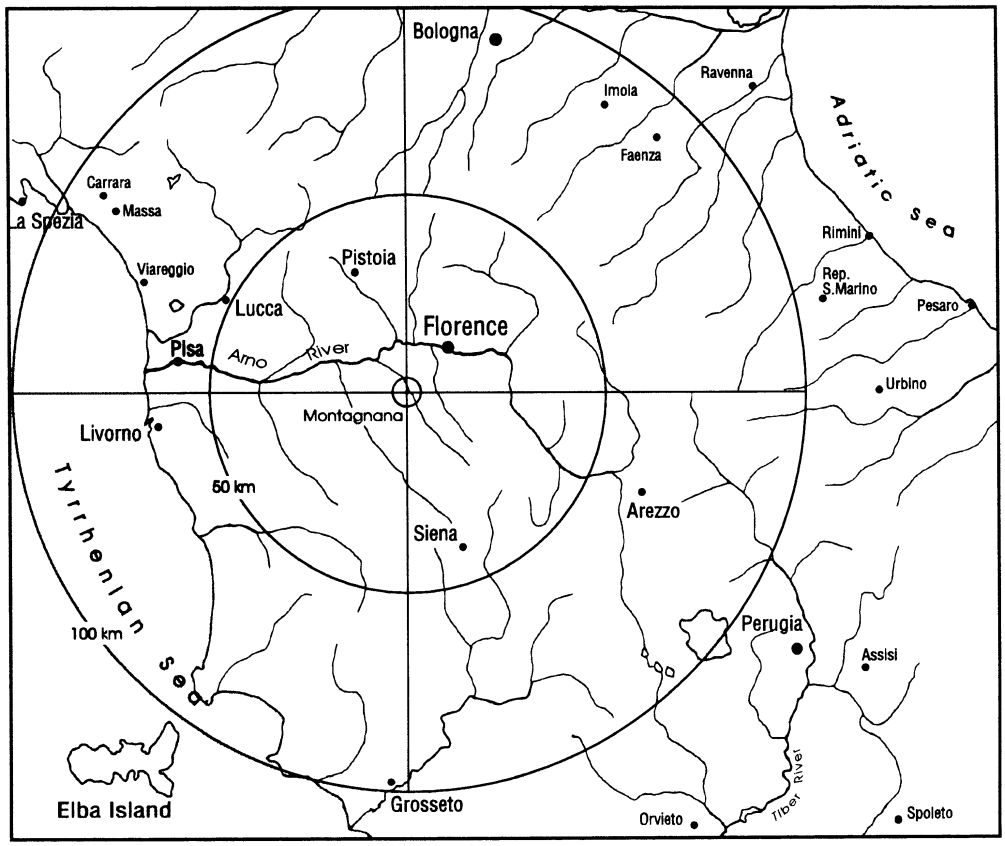

Fig. 2. – Regional map with the Polar 55C radar location.

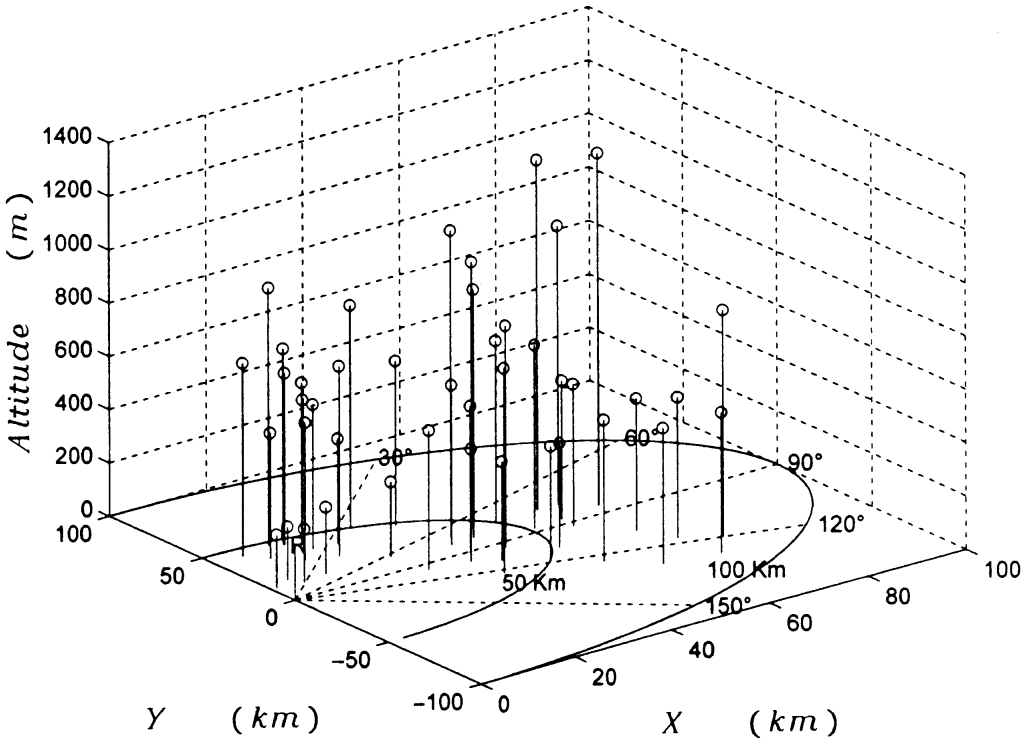

Fig. 3. – The location and the altitude of rain gauges with respect to the radar.

processed by a SP20 radar signal processor (manufactured by Lassen Research, USA) which is capable of providing real time estimates of reflectivity at horizontal polarization (Z_H) and the differential reflectivity (Z_{DR}). More details about the radar can be found in Scarchilli *et al.* [9]. The Arno river basin was also instrumented with a network of tipping bucket rain gauges. The rain gauge network was operated by the "Servizio Idrografico e Mareografico« of Pisa, Italy. The rainfall accumulation in the rain gauges was recorded every 15 minutes with a resolution of 0.2 mm. The rain gauges were distributed throughout the basin with the closest being 12 km and the farthest being 90 km from the radar. The experimental region is a mountainous terrain and therefore the rain gauges were at various altitudes ranging between sea level and 1400 meters. Figure 3 shows the location and the altitude of the rain gauges with respect to the radar.

The data presented in this paper were collected during a meteorological event that occurred on October 30 and 31, 1992 over central Italy. The event was associated with the passage of a frontal perturbation that originated on the southern Mediterranean areas and moved towards north, northeast; that was characterized by the presence of very unstable masses of warm moist air. The storm associated with this event produced intense rainfall over the Arno river basin, creating flood warnings in some of the rivers in the Arno river basin. During this event the Polar 55C was put on an "operational mode" to monitor the basin for hydrological application. This mode consisted of PPI scan strategy done over full 360 degrees in azimuth at a fixed elevation angle with

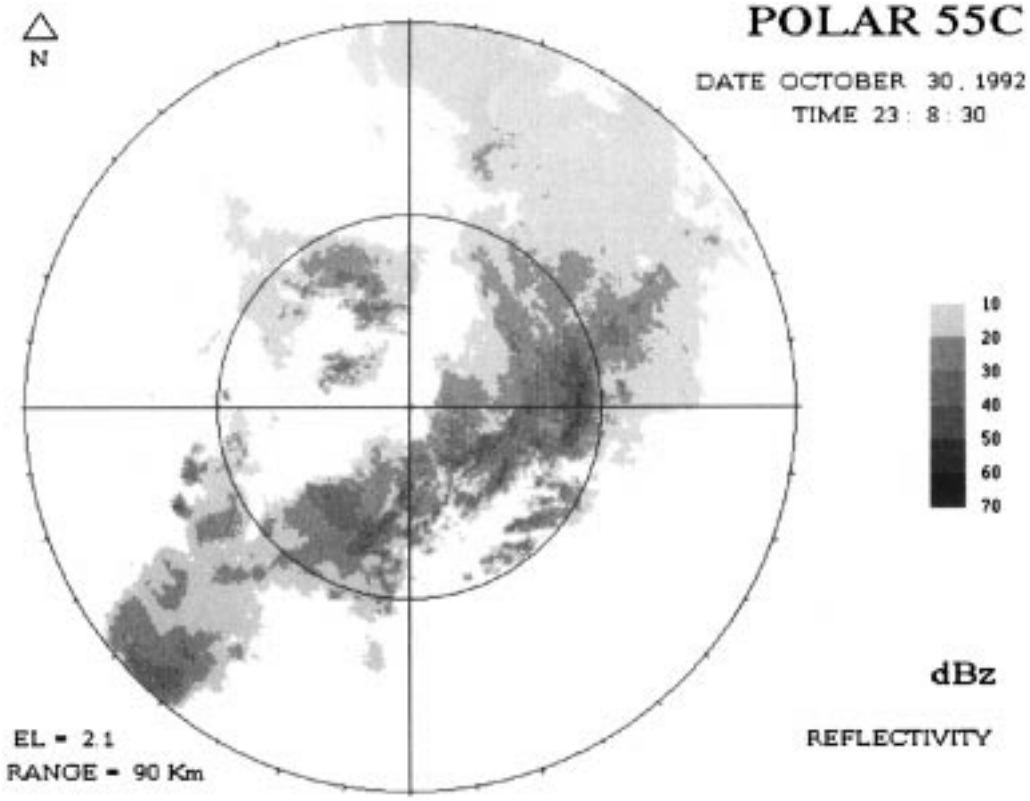

Fig. 4. – A typical PPI of the reflectivity data observed during the precipitation event of 30-31 October 1992.

routine time intervals. Because of the excessive ground clutter in the area, the elevation angle was chosen to be 1.8 degrees. The melting layer of the storm was at 2.8 km, and therefore most of the radar measurements were in the rain phase of the storms. The time interval between scans was set to be 10 minutes to sample the storm system adequately. Figure 4 shows a typical PPI of the reflectivity data from the storm. The radar measurements were obtained integrating 64 sample pairs of the radar returns with a pulse repetition time of 0.85 ms. The archived parameters were the reflectivity at horizontal polarization, the differential reflectivity, the mean Doppler velocity and spectral Doppler width.

Radar PPIs are obtained nearly instantaneously whereas rain gauge data are obtained as accumulation over finite time intervals. With a scan rate of 6 degrees/s it takes 1 minute to get a PPI, whereas the rain gauge data in this data set is integrated over 15 minutes. Therefore, to enable proper comparison between radar and rain gauge data, the following procedure is adopted: a time series of radar data was constructed at the rain gauge locations from the instantaneous snapshots of the PPIs, and then this time series was interpolated to provide the time synchronization between the radar and rain gauge data. Figure 5 shows a sample time series of rainfall constructed for a rain gauge and the corresponding radar estimate R_{ZH} at the rain gauge location.

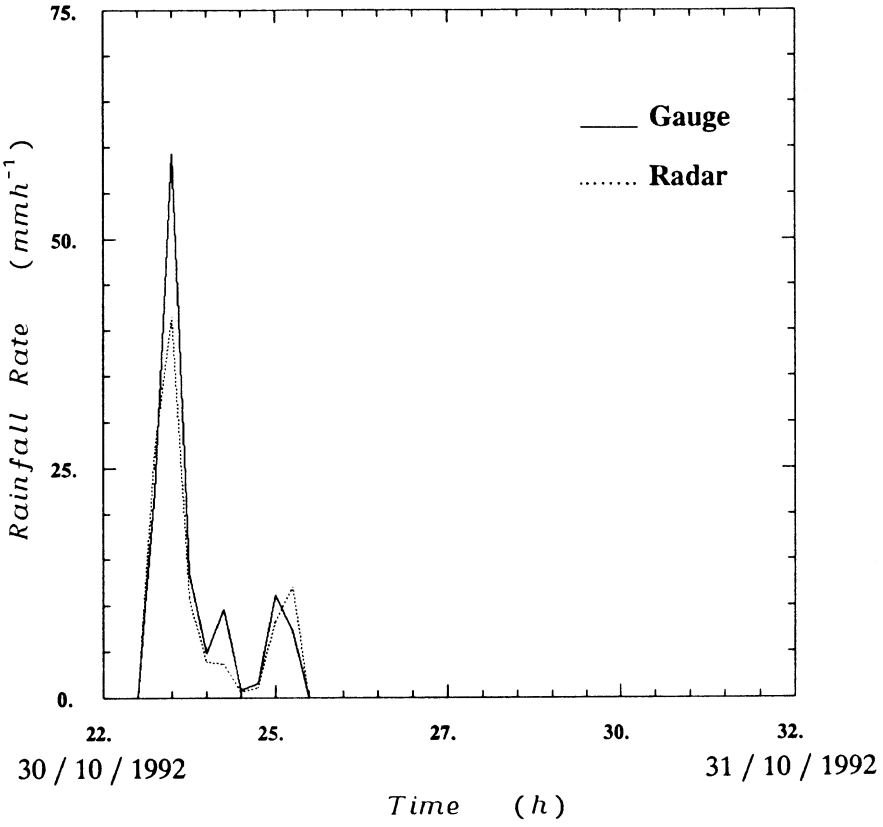

Fig. 5. – Sample time series of rainfall constructed for rain gauge (Il Palagio) and the corresponding radar estimate R_{ZH}.

One additional point of concern with *C*-band radar data in rain is attenuation. It is well established that *C*-band radar signals undergo non-negligible attenuation and differential attenuation in rainfall. Thus, to be able to use the data successfully, it should be corrected for attenuation. Correction for attenuation can be done either from reflectivity and Z_{DR} [10] or using differential propagation phase [4, 11] depending upon the measurement parameters that are available. A cumulative attenuation correction procedure based on Z_H and Z_{DR} is applied here [12]; this procedure is a simplified version of the technique suggested by Aydin *et al.* [10].

3. – Dual polarization rainfall estimates

The distribution of raindrop size and shape forms the building block for obtaining the properties of the rain medium such as the reflectivity Z, the rainfall rate R and the differential reflectivity Z_{DR}. The gamma distribution model can adequately describe many of natural variations in the raindrop size distribution (RSD) [13]. This model is

given by

$$N(D) = N_0 D^{\mu} \exp\left[\frac{-(3.67+\mu)\,D}{D_0}\right], \tag{1}$$

where N_0, D_0 and μ are the parameters of the RSD. The rainfall rate R and the radar parameters such as the reflectivity factors at horizontal and vertical polarization $Z_{\mathrm{H,V}}$ and Z_{DR} can be expressed in terms of the RSD as follows:

$$R = 0.6\pi \times 10^{-3} \int D^3 N(D)\, v(D)\, \mathrm{d}D\,, \tag{2}$$

where $v(D)$ is the terminal fallspeed in still air.

$$Z_{\mathrm{H,V}} = \frac{\lambda^4}{\pi^5 |K|^2} \int \sigma_{\mathrm{H,V}}(D)\, N(D)\, \mathrm{d}D\,, \tag{3}$$

$$Z_{\mathrm{DR}} = 10\, \log\left(\frac{Z_{\mathrm{H}}}{Z_{\mathrm{V}}}\right), \tag{4}$$

see Seliga and Bringi [3].

Utilizing the radar observables Z_{H} and Z_{DR}, two estimates of rainfall rate R can be obtained as follows [14]:

$$R_{\mathrm{ZH}} = C_{\mathrm{ZH}} Z_{\mathrm{H}}^{\nu}, \tag{5}$$

$$R_{\mathrm{DR}} = C_{\mathrm{DR}} Z_{\mathrm{H}}^{\alpha} 10^{\beta Z_{\mathrm{DR}}}, \tag{6}$$

where C_{ZH}, C_{DR}, ν, α and β depend on the operating wavelength. Gorgucci *et al.* [14] have derived the dual polarization rainfall algorithm at *C*- and *S*-band frequencies based on simulation as

$$R_{\mathrm{DR}}^{C} = 7.60 \times 10^{-3} Z_{\mathrm{H}}^{0.93} 10^{-0.281 Z_{\mathrm{DR}}}\,, \tag{7a}$$

$$R_{\mathrm{DR}}^{S} = 10 \times 10^{-3} Z_{\mathrm{H}}^{0.92} 10^{-0.369 Z_{\mathrm{DR}}}\,, \tag{7b}$$

However, the same simulation can be used to get representative *Z*-*R* relations and they are given by

$$R_{\mathrm{ZH}}^{C} = 2.71 \times 10^{-2} Z_{\mathrm{H}}^{0.71}\,, \tag{8a}$$

$$R_{\mathrm{ZH}}^{S} = 11.9 \times 10^{-2} Z_{\mathrm{H}}^{0.58}\,. \tag{8b}$$

The algorithms given by (7) and (8) as well as the Marshall-Palmer rainfall algorithm,

$$R_{\mathrm{MP}} = 3.65 \times 10^{-2} Z_{\mathrm{H}}^{0.625} \tag{9}$$

are used throughout the various procedures in this paper. We note here that in the above equations Z_{H} is in units of $\mathrm{mm}^6\ \mathrm{m}^{-3}$ and Z_{DR} is in dB.

4. – Parametric estimates of rainfall rate

4·1. *Pointwise radar and rain gauge comparison.* – The procedure to compute point rainfall using radar and rain gauge is conceptually straightforward but numerous details are important. We want to stress here that we have not made any adjustment for storm movement, or any another adjustment or fine tune of the data and the comparison is direct. The actual steps involved in collecting radar data for each rain gauge location are as follows: *a*) the location of each rain gauge is mapped on the radar PPI of reflectivity factor and differential reflectivity, *b*) the radar data are converted to rainfall rate using each of the algorithms described in the previous section, *c*) the radar estimates are then averaged over nearest neighbors of one km each side centered at the rain gauge location in order to smooth the data over measurement errors. The rainfall obtained from radar over time is then accumulated for the entire precipitation event.

We have also estimated a figure of merit to quantitatively describe the capability of algorithms to estimate rainfall, namely the Fractional Standard Error (FSE) defined as

$$\text{FSE} = \frac{\langle[\text{Rainfall (radar)} - \text{Rainfall (Gage)}]^2\rangle^{0.5}}{\langle\text{Rainfall (Gage)}\rangle} \tag{10}$$

where $\langle\ \rangle$ represents the expected value.

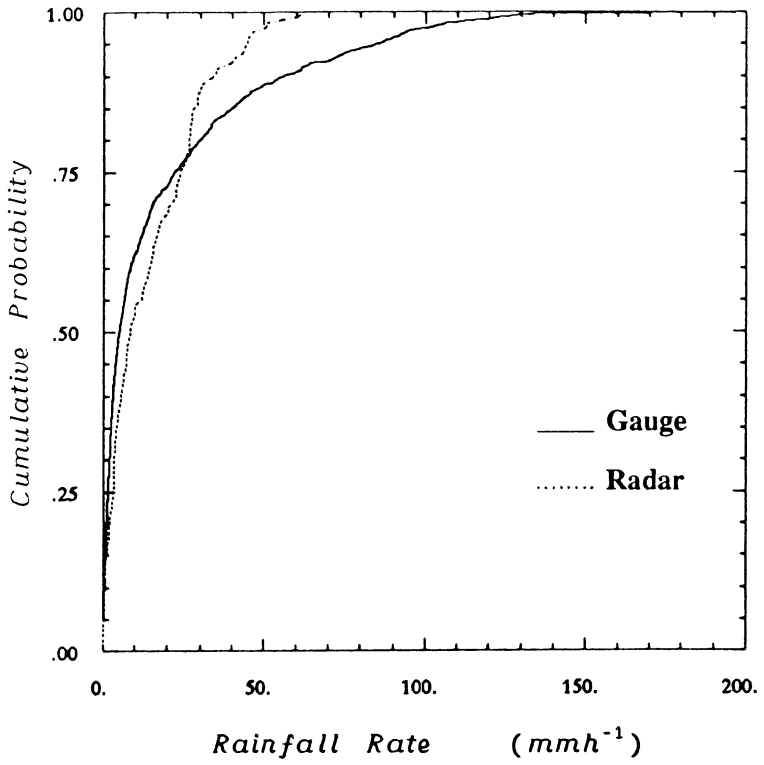

Fig. 6. – The experimental probability distribution function of rainfall. The solid line shows the CDF observed by rain gauge whereas the dotted line shows the CDF obtained from radar data using Marshall-Palmer *Z-R* relation.

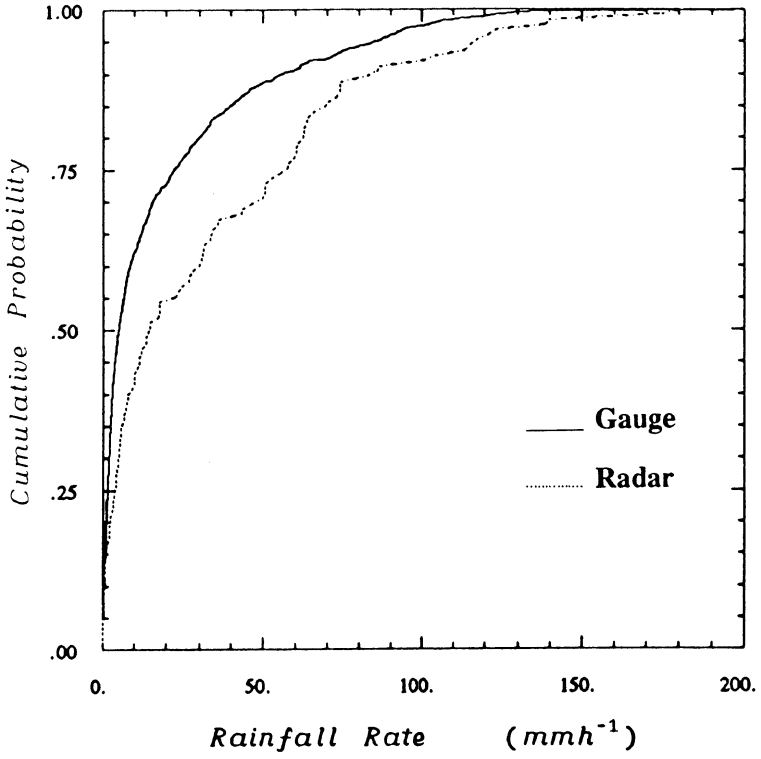

Fig. 7. – The experimental probability distribution function of rainfall. The solid line shows the CDF observed by rain gauge whereas the dotted line shows the CDF obtained from the *S*-band radar data using R_{ZH} given by (8*b*).

4·2. *Cumulative distribution function* (CDF) *matching procedure*. – The CDF of rainfall can be constructed from radar and the functional shape will depend on the type of algorithm used to convert the radar observations to rainfall. The rainfall conversion algorithm can be either *Z-R* algorithm or multiparameter-based algorithm. The *Z-R* and the multiparameter algorithms have the following forms:

$$R_{ZH} = C_1 Z_H^{\alpha}, \tag{11}$$

$$R_{DR} = C_2 Z^{\beta} 10^{-\nu Z_{DR}}, \tag{12}$$

where C_1, α, C_2, β and ν are the parameters of the algorithm. Our procedure for estimating the parameters of the radar rainfall algorithm based on CDF matching is as follows:

I) For a given starting guess of parameters C_1, α, C_2, β and ν evaluate the radar rainfall estimate at each rain gauge location as described in sect. **3**. Typically, the initial guess is based on established relations given by (7) and (8).

II) Construct the CDF based on the result of step I).

III) Construct the CDF based on rain gauge observations.

IV) Construct the Sum Square Error (SSE) between the radar-based and rain

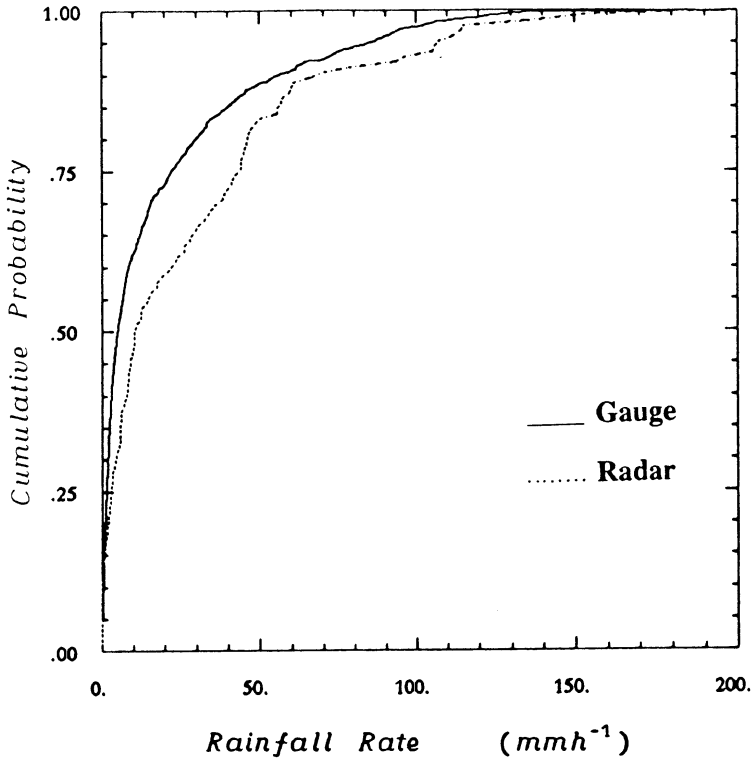

Fig. 8. – The experimental probability distribution function of rainfall. The solid line shows the CDF observed by rain gauge whereas the dotted line shows the CDF obtained from the *S*-band radar data using R_{ZH} given by (7*b*).

gauge-based CDF, obtained as integration of the square deviation between the two CDFs over the entire range.

V) Iterate the coefficients to minimize the sum square error.

For *S*-band, figs. 6, 7, 8 show comparisons of the CDF of rainfall obtained from rain gauge and radar using Marshall-Palmer, *Z-R* relation and the multiparameter algorithm given by (9), (8*b*) and (7*b*), respectively. Figures 9, 10 and 11 show similar comparison for the *C*-band. The CDFs were obtained using data from all the rain gauges. The corresponding sum square error between the two CDFs in self-consistent units is shown in table II for *S*-band and table III for *C*-band.

To obtain the optimum *Z-R* and multiparameter relations, we need to note here that the procedure is done using nonlinear optimization algorithms. We do not linearize the *Z-R* relation or R_{DR} taking logarithms. The linearization procedure taking logarithms disturbs the natural distribution of rainfall in the minimization process. At the *S*-band the resulting parameter estimates for R_{ZH} and R_{DR} based on CDF matching criteria are as follows:

$$R^{S}_{ZH}(\mathrm{CDF}) = 12.3\times 10^{-2} Z_H^{0.572}, \tag{13}$$

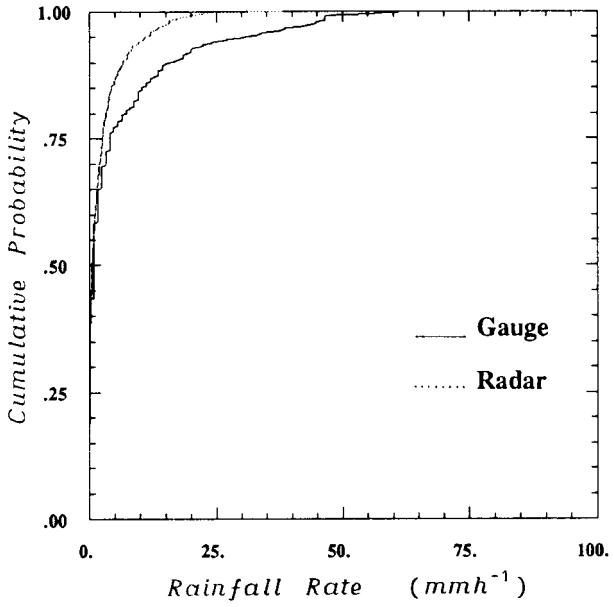

Fig. 9. – The experimental probability distribution function of rainfall. The solid line shows the CDF observed by rain gauge whereas the dotted line shows the CDF obtained from radar data using Marshall-Palmer Z-R relation.

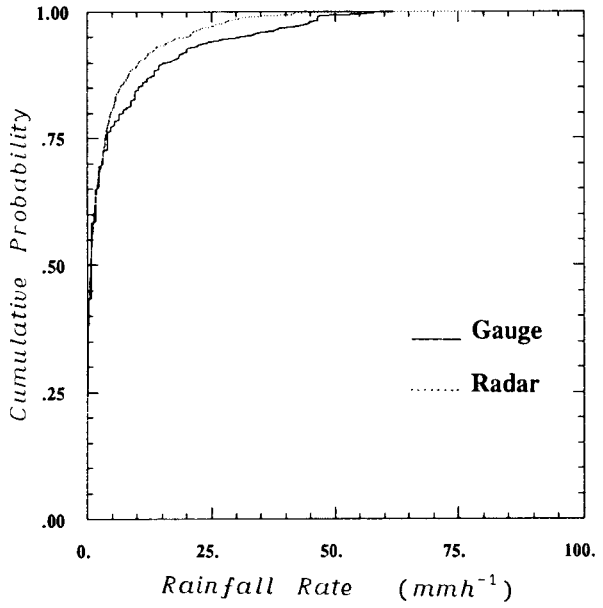

Fig. 10. – The experimental probability distribution function of rainfall. The solid line shows the CDF observed by rain gauge whereas the dotted line shows the CDF obtained from the C-band radar data using R_{ZH} given by (8a).

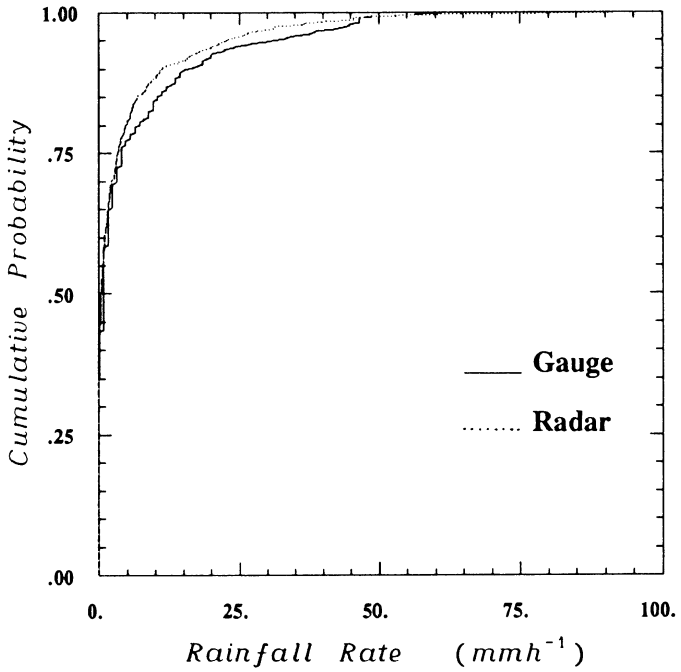

Fig. 11. – The experimental probability distribution function of rainfall. The solid line shows the CDF observed by rain gauge whereas the dotted line shows the CDF obtained from the *C*-band radar data using R_{ZH} given by (7*b*).

with the corresponding SSE = 380, and

$$R^{S}_{DR}(\mathrm{CDF}) = 10 \times 10^{-3} Z_{H}^{0.914} 10^{-0.377 Z_{DR}}, \tag{14}$$

with the corresponding SSE = 130.

The results for the *C*-band are

$$R^{C}_{ZH}(\mathrm{CDF}) = 4.07 \times 10^{-2} Z_{H}^{0.71}, \tag{15}$$

with the corresponding SSE = 130, and

$$R^{C}_{DR}(\mathrm{CDF}) = 1.80 \times 10^{-2} Z_{H}^{0.88} 10^{-0.374 Z_{DR}}, \tag{16}$$

with the corresponding SSE = 108.

TABLE II. – *Sum Square Error* (SSE) *between the radar-based and the rain gauge-based Cumulative Distribution Function* (CDF) *at the S-band.*

	SSE
R_{MP}	560
R_{ZH}	401
R_{DR}	167

TABLE III. – *Sum Square Error* (SSE) *between the radar-based and the rain gauge-based Cumulative Distribution Function* (CDF) *at the C-band.*

	SSE
R_{MP}	930
R_{ZH}	317
R_{DR}	253

There are three important observations we can make from the results obtained from (13)-(16). Firstly, the optimum Z-R relation matching the CDF is different from the Marshall-Palmer algorithm or any other standard Z-R algorithm. Secondly, the best multiparameter algorithm based on (Z_H, Z_{DR}) has a lower SEE compared to the best Z-R relation, thereby indicating that in a CDF matching procedure to rainfall estimation, polarimetric techniques have some improvement to offer. The third significant conclusion of practical importance at the S-band is that the optimum R_{DR}(CDF) has parameters and error structure fairly close to the theoretical algorithm, indicating thereby that we can possibly do with just one expression.

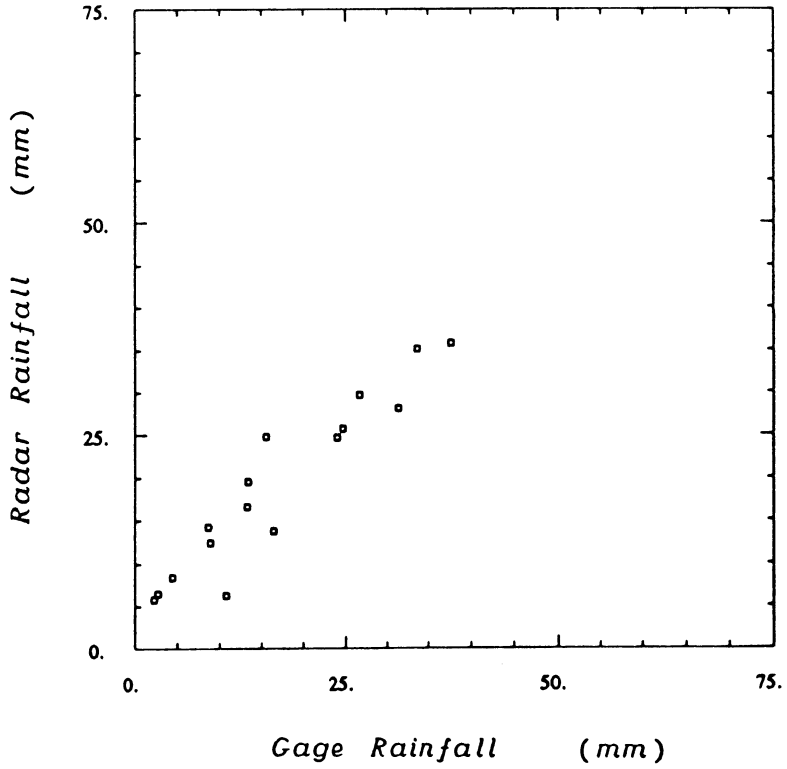

Fig. 12. – Scatter plot between rainfall accumulation at TRMM rain gauge location and the corresponding rainfall accumulation obtained from the S-band radar estimates R_{ZH}(CDF), given by (13).

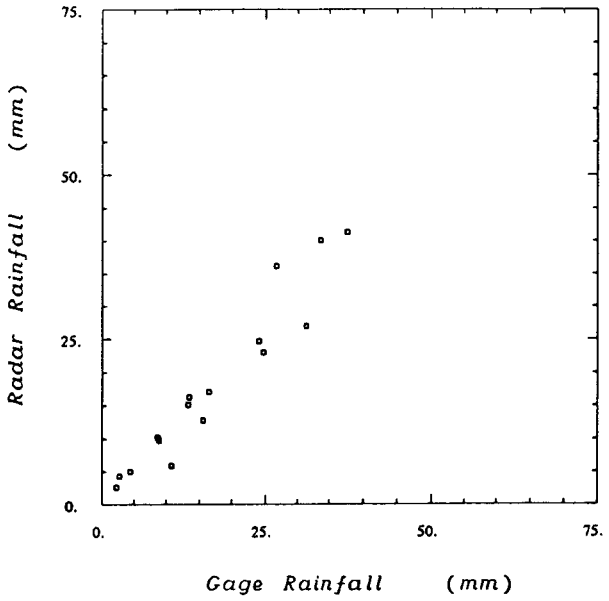

Fig. 13. – Scatter plot between rainfall accumulation at TRMM rain gauge location and the corresponding rainfall accumulation obtained from the *S*-band radar estimates R_{DR}(CDF), given by (14).

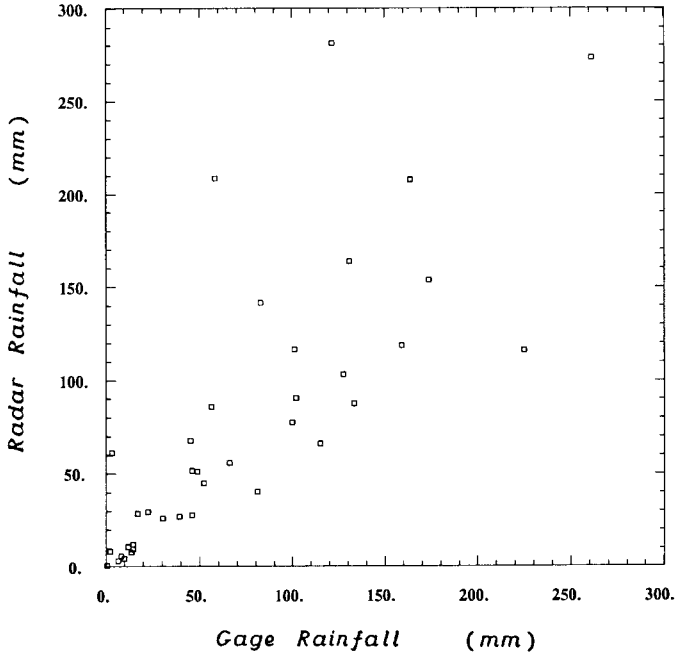

Fig. 14. – Scatter plot of rainfall accumulation at rain gauge location and the corresponding rainfall accumulation obtained from the *C*-band radar estimates R_{ZH}(CDF), given by (15).

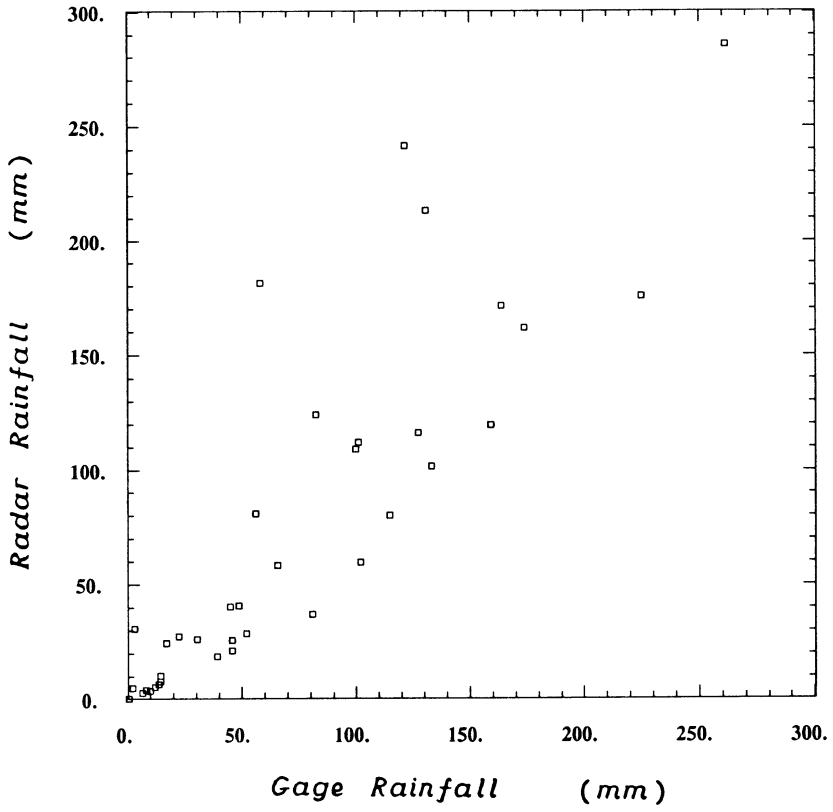

Fig. 15. – Scatter plot of rainfall accumulation at rain gauge location and the corresponding rainfall accumulation obtained from the *C*-band radar estimates R_{DR}(CDF), given by (16).

The algorithms for *S*- and *C*-band are different primarily because of the frequency of operation.

The algorithms given by (13) and (16) have been obtained in a statistical framework for radar and raing gauge comparison. The rainfall accumulation at rain gauge location is then compared using the procedure similar to the analysis done in sect. **3**.

Figures 12 and 13 show the scatter plot of rainfall accumulation at TRMM rain gauge locations based on R_{ZH}(CDF) and R_{DR}(CDF) obtained using the procedure described in Sect. **3** but substituting the recomputed algorithms (13) and (14). The standard error of fig. 12 based on R_{ZH}(CDF) is 25%, whereas the corresponding standard error for R_{DR}(CDF) is 21% (fig. 13). Note here that the minimization and error computation are done on the same data set that was used to obtain the parameters. However, even under such conditions the best R_{DR}(CDF) seems to have a slight edge over the best R_{ZH}(CDF). For *C*-band the total standard error based on R_{ZH}(CDF) is 66% (fig. 14), whereas the corresponding standard error for R_{DR}(CDF) is 53% (fig. 15). In general the standard errors are expected to be slightly higher.

5. – Summary and conclusions

Two general approaches to remotely estimate rainfall with radar are studied here, namely:

a) obtain instantaneous point estimates of ranfall,

b) statistical techniques applied in a mean sense for the whole storm, or climatological region.

Conventionally, multiparameter radar estimates of rainfall have taken the first approach and have been primarily associated with accounting for the variability in the drop size distribution, whereas the statistical techniques have used only reflectivity. This paper presents the use of multiparameter radar measurements in a statistical framework for estimating rainfall. We have used data from a rain event during CaPE at the *S*-band and from an intense rainfall over the Arno river basin at the *C*-band, to test the analytical procedures developed in this paper. Pointwise comparison of rainfall accumulation at the rain gauge sites using multiparameter estimate R_{DR} was found to have a standard error of 35%, whereas the Marshall-Palmer Z-R relations were found to have a standard error of 49% for the CaPE data. Pointwise comparison at the *C*-band over the Arno river basin showed that the R_{MP} had a FSE of 84%, the R_{ZH} algorithm described in our paper had a FSE of 64% and the Z_{DR}-based R_{DR} algorithm had a FSE of 59%. The difference in the error percentages between the two frequencies can be attributed to ground clutter and attenuation problems at the *C*-band.

We have analyzed the difference between the experimental CDF obtained from radar and rain gauge network. For CaPE data, such an analysis showed that Marshall-Palmer and Z-R relations had a sum square error (in self-consistent scale) of 560 and 401, respectively, whereas the theoretical R_{DR} had an error of 167. Similar analysis for the *C*-band radar data over the Arno river basin showed that Marshall-Palmer and Z-R relations had a sum square error (in self-consistent scale) of 930 and 317, respectively, whereas the theoretical R_{DR} had an error of 253.

We have subsequently obtained parametrization for the R_{DR} and Z-R algorithms matching the experimental CDF of rainfall from radar to the one that is observed by rain gauge. This analysis showed that R_{DR} can be parametrized to obtain better match between the experimental CDF of rainfall obtained by radar and rain gauge network. The best match between the radar and rain gauge CDF was obtained for R_{DR} relations not very different from the theoretical relations given by (7*a*) and (7*b*). In addition, the best Z-R relation defined as the one that minimizes the difference between radar and rain gauge network based CDFs had a SSE of 380 (in self-consistent scale) higher than the theoretical R_{DR} relation for CaPE data. At the *C*-band the best Z-R relation had a sum square error of 130 while the R_{DR} estimate obtained by CDF procedure has the corresponding sum square error of 108. Utilizing the parametrizations obtained from the CDF matching procedure and comparing with rain gauge measurements yielded standard errors of 25% and 21%, respectively for R_{ZH} and R_{DR} for CaPE data; for the *C*-band the standard errors were 66% and 53% for R_{ZH} and R_{DR}, respectively. In summary, it appears from this analysis that multiparameter radar algorithms can be obtained from the CDF matching procedure, that can provide more accurate estimates of rainfall at ground in comparison to any Z-R algorithm.

* * *

This research was supported by the EEC Program on the Environment "Storm '93" (PL910060: EC-1991-94, IFA-CNR), by the National Group for Defence from Hydrogeological Hazards (CNR, Italy) and by ASI (n. 94-RS-10), by NASA and the NSF (ATM-9200761) (CSU). The CaPE program was a cooperative multi-agency field program sponsored by the National Science Foundation (NSF), Federal Aviation Administration (FAA), National Aeronautics and Space Administration (NASA), National Oceanic and Atmospheric Administration (NOAA) and the United States Airforce (USAF). The authors acknowledge Prof. D. GIULI, Drs. L. FACHERIS, L. BALDINI, and E. PALMISANO for their collaborative effort in the radar program. The authors would like to offer special thanks to G. VEZZANI, A. VOLPI and P. MERENDINO of SMA who provided the technical support during the collection of radar data. The authors are grateful to P. IACOVELLI for assistance rendered during the preparation of the manuscript.

REFERENCES

[1] CALHEIROS R. V. and ZAWADZKI I., *Reflectivity-rain rate relationships for radar hydrology in Brazil*, *J. Clim. Appl. Meteor.*, **26** (1987) 118.
[2] AYDIN K., LURE Y. M. and SELIGA T. A., *Polarimetric radar measurements of rainfall compared with ground-based rain gauges during MAYPOLE '84*, *IEEE Trans. Geosci. Remote Sens.*, **28** (1990) 443.
[3] SELIGA T. A. and BRINGI V. N., *Potential use of the radar reflectivity at orthogonal polarizations for measuring precipitation*, *J. Appl. Meteorol.*, **15** (1976) 69.
[4] SCARCHILLI G., GORGUCCI E., CHANDRASEKAR V. and SELIGA T. A., *Rainfall estimation using polarimetric techniques at C-Band frequencies*, *J. Appl. Meteorol.*, **32** (1993) 1150.
[5] BRINGI V. N., DETWILER A., CHANDRASEKAR V., SMITH P. L., LIU L., CAYLOR I. J. and MUSIL D., *Multiparameter radar and aircraft study of the transition from early to mature storm during CaPE: The case of 9 August 1991*, Preprints, *26th Radar Meteorology Conference, Norman* (American Meteorology Society) 1993, pp. 318-320.
[6] CHANDRASEKAR V. and BRINGI V. N., *Error structure of multiparameter radar and surface measurements of rainfall. Part I: Differential reflectivity*, *J. Atmos. Ocean. Technol.*, **5** (1988) 783.
[7] ZAWADZKI I., *Factors affecting the precision of radar measurements of rain*, Preprints, *22nd Radar Meteorology Conference, Zurich* (American Meteorology Society) 1984, pp. 251-256.
[8] FOOTE G. B., Scientific Overview and Operations Plan. National Center for Atmospheric Research, Boulder, Colo. (1991).
[9] SCARCHILLI G., GORGUCCI E., GIULI D., FACHERIS L., FRENI A. and VEZZANI G., *Arno project: Radar system and objectives*, *25th AMS Radar Meteorology Conference, Paris, France* (American Meteorology Society) 1991, pp. 805-808.
[10] AYDIN K., ZHAO Y. and SELIGA T. A., *Rain-induced attenuation effects on C-band dual-polarization meteorological radars*, *IEEE Trans. Geosci. Remote Sens.*, **27** (1989) 57.
[11] BRINGI V. N., CHANDRASEKAR V., BALAKRISHNAN N. and ZRNIC D. S., *An examination of propagation effects in rainfall on radar measurements at microwave frequencies*, *J. Atmos. Ocean. Technol.*, **7** (1990) 829.
[12] GORGUCCI E., SCARCHILLI G. and CHANDRASEKAR V., *Radar and raingage measurements of rainfall over the Arno basin*, Preprints, *Conference on Hydrology, Dallas, Texas* (1995), pp. 68-73.
[13] ULBRICH C. W., *Natural variations in the analytical form of raindrop size distributions*, *J. Clim. Appl. Meteor.*, **22** (1983) 1764.
[14] GORGUCCI E., SCARCHILLI G. and CHANDRASEKAR V., *A robust estimator of rainfall rate using differential reflectivity*, *J. Atmos. Ocean. Technol.*, **11** (1994) 586.